To appear in *The Astrophysical Journal*

Search for a Point-Source Counterpart of the Unidentified Gamma-Ray Source TeV J2032+4130 in Cygnus

R. Mukherjee[1], J. P. Halpern[2,3], E. V. Gotthelf[3], M. Eracleous[4,5], N. Mirabal[2]

ABSTRACT

We have made a multiwavelength study of the overlapping error boxes of the unidentified γ-ray sources TeV J2032+4130 and 3EG J2033+4118 in the direction of the Cygnus OB2 association ($d = 1.7$ kpc) in order to search for a point-source counterpart of the first unidentified TeV source. Optical identifications and spectroscopic classifications for the brighter X-ray sources in *ROSAT* PSPC and *Chandra* ACIS images are obtained, without finding a compelling counterpart. The classified X-ray sources are a mix of early and late-type stars, with one exception. The brightest source in the *Chandra* observation is a new, hard absorbed source that is both transient and rapidly variable. It lies $7'$ from the centroid of the TeV emission, which places it outside of the claimed 2σ location ($r \approx 4\farcm8$). A possible eclipse or "dip" transition is seen in its light curve. With a peak 1–10 keV luminosity of $\approx 7 \times 10^{32}\,(d/1.7\,\mathrm{kpc})^2$ ergs s^{-1}, this source could be a quiescent low-mass X-ray binary that lies beyond the Cyg OB2 association. A coincident, reddened optical object of $R = 20.4$, $J = 15.4$, $H = 14.2$, and $K = 13.4$ is observed, but not yet classified due to the lack of obvious emission or absorption features in its spectrum. Alternatively, this *Chandra* and optical source might be a considered a candidate for a "proton blazar," a long hypothesized type of radio-weak γ-ray source. More detailed observations will be needed to determine the nature of this variable X-ray source, and to assess the possibility of its connection with TeV J2032+4130.

[1]Department of Physics & Astronomy, Barnard College, New York, NY 10027

[2]Department of Astronomy, Columbia University, New York, NY 10027

[3]Columbia Astrophysics Laboratory, Columbia University, New York, NY 10027

[4]Department of Astronomy & Astrophysics, The Pennsylvania State University, University Park, PA 16802

[5]Visiting Astronomer, Kitt Peak National Observatory, National Optical Astronomy Observatories, which is operated by the Association of Universities for Research in Astronomy, Inc. (AURA) under cooperative agreement with the National Science Foundation.

Subject headings: gamma-rays: individual (3EG J2033+4118, TeV J2032+4130) — gamma-rays: observations — X-rays: stars

1. Introduction

The serendipitous detection of emission coming from the direction of the Cygnus OB2 stellar association by the HEGRA CT-System at La Palma (Daum et al. 1997) represents the first discovery of an unidentified TeV source, extending the mystery of the elusive γ-ray sources to the TeV regime. TeV J2032+4130 was discovered (Aharonian et al. 2002a) in observations originally devoted to Cygnus X–3 and the unidentified EGRET (Energetic Gamma-ray Experiment Telescope) source GeV J2035+4214 (Lamb & Macomb 1997). An analysis of these combined fields led to the detection of a source at (J2000) $20^{\rm h}32^{\rm m}07^{\rm s} \pm 9\overset{\rm s}{.}2_{\rm stat} \pm 2\overset{\rm s}{.}2_{\rm sys}$, $+41°30'30'' \pm 2\overset{\prime}{.}0_{\rm stat} \pm 0\overset{\prime}{.}4_{\rm sys}$. Its error circle overlaps the edge of the 95% confidence error ellipse of another EGRET source, 3EG J2033+4118, and is $\approx 0\overset{\circ}{.}5$ north of Cyg X–3. It is not clear if TeV J2032+4130 is associated with 3EG J2033+4118, which is itself of uncertain origin. There is some evidence that the TeV emission is extended, with a Gaussian 1σ radius of $\sim 5\overset{\prime}{.}6 \pm 1\overset{\prime}{.}7$. Unlike the flaring blazars that have been detected so far, TeV J2032+4130 was found to be steady in repeated HEGRA observations from 1999 to 2001. The integrated flux measured above 1 TeV was found to be $(4.5 \pm 1.3_{\rm stat}) \times 10^{-13}$ photons cm^{-2} s^{-1}, which is $\approx 2.6\%$ of the flux of the Crab Nebula (Aharonian et al. 2002a).

The majority of the γ-ray sources detected above 100 MeV by the EGRET instrument on the *Compton Gamma Ray Observatory* (CGRO) are unidentified, some remaining so since the first surveys of the γ-ray sky with the COS–B satellite. Resolving the nature of these mysterious γ-ray sources is a challenge across all wavelengths. Their relatively large error boxes make counterpart searches difficult. Unidentified EGRET sources typically have positional uncertainties of $\sim 0\overset{\circ}{.}5 - 1°$, making identification on the basis of position alone nearly impossible, especially in the Galactic plane. We have found that multiwavelength studies of EGRET fields on a case-by-case basis are often useful in finding a likely identification. Such an approach has been used to suggest counterparts for the EGRET unidentified sources 2EG J0635+0521 (Kaaret et al. 1999), 3EG J2227+6122 (Halpern et al. 2001a), 3EG J1835+5918 (Halpern et al. 2002; Mirabal et al. 2000,2001), 3EG J2006–2321 (Wallace et al. 2002), 3EG J2016+3657 (Mukherjee et al. 2000; Halpern et al. 2001b), 3EG J1621+8203 (Mukherjee et al. 2002), and 3EG 2021+3716 (Roberts et al. 2002), to name a few examples (see the review by Caraveo 2002).

Imaging atmospheric Cherenkov telescopes (IACTs) like HEGRA have the advantage of much better angular resolution, and therefore smaller error boxes for γ-ray source positions

in comparison to EGRET. In this paper, we adopt for the moment the hypothesis that TeV J2032+4130 is *not* significantly extended, in which case one should search for and evaluate candidate point-source counterparts at other wavelengths. Accordingly, we studied the EGRET source 3EG J2033+4118, archival radio data from the NRAO-VLA Sky Survey (NVSS: Condon et al. 1998), and pointed *ROSAT* X-ray observations of the field of 3EG J2033+4118 and TeV J2032+4130. We also examined a recent *Chandra* observation that was centered on the TeV source, and obtained optical identifications of the brightest X-ray sources in this region using the MDM Observatory, Kitt Peak National Observatory (KPNO), and the *Hobby-Eberly Telescope* (*HET*).

2. Gamma-ray Observations of 3EG J2033+4118

The EGRET source 3EG J2033+4118 is located at $l = 80.^\circ27$, $b = +0.^\circ73$ (Hartman et al. 1999), with a 95% error ellipse defined by semi-major and semi-minor axes of $0^\circ.31$ and $0^\circ.25$, respectively (Mattox, Hartman, & Reimer 2001). Figure 1 shows the 95% confidence EGRET ellipse superimposed on a *ROSAT* X-ray image that is described further in §3. 3EG J2033+4118 was detected by EGRET in several viewing periods, with the most significant detection in 1993 March (VP 212). Figure 2 shows the light curve measured by EGRET during 1991–1997. The points before 1996 come from the Third EGRET Catalog (3EG, Hartman et al. 1999), in which the summed exposure has a flux above 100 MeV of $(73.0 \pm 6.7) \times 10^{-8}$ photons cm^{-2} s^{-1}. The corresponding background-subtracted spectrum of 3EG J2033+4118 is hard, with a photon spectral index of 1.96 ± 0.10 (Hartman et al. 1999).

This location was also in the EGRET field of view four times after the 3EG catalog. For two of these the source was almost 30° from the axis, so we exclude them. The remaining two detections are 2.4σ and 4.2σ. Their fluxes are shown as the last two points in Figure 2. A chi-square analysis was used to calculate the "variability index" defined by McLaughlin et al. (1996). This index is sometimes used to judge variability in EGRET sources, although it is somewhat arbitrary. The variability index of 3EG J2033+4118 was found to be $V = 1.4$. For comparison, McLaughlin et al. (1996) interpret $V < 0.5$ as non-variable and $V \geq 1.0$ as variable.

3. X-ray and Radio Observations

Figure 1 shows an X-ray image taken with the *ROSAT* Position Sensitive Proportional Counter (PSPC) in the energy range 0.2–2.0 keV, covering the field of 3EG J2033+4118/TeV

J2032+4130. This image was created by co-adding exposure-corrected skymaps of 23.5 ks of data taken during 1991 and 1993. These fields were targeted originally to include the Cyg OB2 association and also Cyg X-3. The EGRET 95% error ellipse for 3EG J2033+4118 is superposed on the image, as is the 1σ error contour of the TeV J2032+4130 centroid position. The larger circle around the TeV position indicates the possible Gaussian 1σ extent of the TeV source (Aharonian et al. 2002a). Figure 3 shows a *ROSAT* HRI image, covering roughly the same field as that shown in Figure 1. The image was created by co-adding exposure corrected skymaps of $\approx$ 155 ks of data taken during observations of Cyg OB2 and Cygnus X-3 in 1993–1995. The sources numbered in Figure 3 correspond to those in Figure 1 and Table 1.

A detailed description of *ROSAT* results on the sources in the Cyg OB2 association is given by Waldron et al. (1998). Several of the stars in the Cyg OB2 association are among the strongest stellar X-ray sources in the Galaxy. In Table 1 we list the coordinates of the brightest ROSAT sources as marked in Figures 1 and 3, along with optical identifications and positions. We have concentrated on obtaining optical identifications of several X-ray sources that are within the region of maximum likelihood for a point source of TeV emission. We find that all of these have ordinary stellar counterparts. Further details on their optical properties are presented in §4.2.

On 2002 August 11, *Chandra* made a 5 ks director's discretionary observation (Butt et al. 2003) of the field of TeV J2032+4130 with the front-illuminated, imaging CCD array of the Advanced CCD Imaging Spectrometer (ACIS-I). Several X-ray sources near the centroid of the TeV source were detected. Figure 4 shows the *Chandra* image with the brightest point sources marked, which are those having at least 10 photons. Their positions and count rates are listed in Table 2. Cross-references to sources detected by both *ROSAT* and *Chandra* are indicated in Tables 1 and 2. The brightest *Chandra* source #2 is notable in that it was *not* detected in any of the *ROSAT* or *Einstein* observations of this field. More details about this source are given in §5.1.

Table 3 is a list of eight 1.4 GHz sources from the NVSS within $10'$ of the TeV centroid. The brightest is an extended source with flux density of only 18 mJy, which is at least an order of magnitude fainter than the weakest candidate radio sources for EGRET blazars considered by Mattox et al. (1999). Furthermore, none of the radio sources is coincident with an X-ray source. Thus, it is unlikely that TeV J2032+4130 has an ordinary blazar counterpart, although new types of blazars can be hypothesized (see §5.3).

4. Optical Observations

4.1. Optical Imaging

In preparation for the identification of X-ray sources in the *Chandra* observation, on 2002 July 7 we obtained a deep R-band image of the field of TeV J2032+4130 using the MDM 1.3m telescope and a thinned, back-illuminated 2048×2048 pixel SITe CCD. This $17' \times 17'$ image covers all of the *Chandra* source positions marked in Figure 4. An astrometric grid was established for the image using 51 stars from the USNO–A2.0 catalog (Monet et al. 1996), with a resulting rms dispersion of $0\farcs49$. Differences between optical and X-ray positions for the most precisely located X-ray sources indicate that the X-ray aspect solution agrees with the USNO–A2.0 reference frame to within $0\farcs5$. Additional images in B, V, R, and I were obtained of the central $9' \times 9'$ of the same field using the MDM 2.4m telescope on 2002 August 23–28.

Likely optical identifications of *Chandra* sources are listed in Table 2, together with approximate R magnitudes from our images or from the USNO–A2.0 where available. Only four of the *Chandra* sources have no optical counterpart to a limiting magnitude > 23. These happen to be the hardest sources in the image, with $> 75\%$ of their photons above 2 keV. Thus they are likely to be AGNs that are highly absorbed by the Galactic ISM, and not, for example, nearby, old neutron stars. A higher-resolution image of the crowded region around *Chandra* source #2 was obtained on the MDM 2.4m telescope on 2002 November 24. Figure 5 shows the possible identification of that source on the 2.4m image.

4.2. Optical Spectroscopy

We obtained complete spectroscopic identifications for all *ROSAT* sources within $10'$ of the centroid of TeV J2032+4130, using the Goldcam spectrograph on the KPNO 2.1m telescope on two runs, in 2002 June and October. The resulting spectra are shown in Figure 6. These are sources *a*, *b*, *c*, *e*, and *f* in Table 1, and all are bright stars. They include one emission-line O star, one dMe star, and three foreground G stars, two of which are also listed in the Massey & Thompson (1991, hereafter MT91) compilation of stars in Cyg OB2. Magnitudes listed in Table 1 are from MT91, or from the USNO–A2.0 catalog (Monet et al. 1996).

A spectrum of the $R \approx 20.4$ counterpart of *Chandra* source #2, also shown in Figure 6, was obtained with the *HET* and Marcario Low Resolution Spectrograph on 2002 December 8. However, its classification remains uncertain as it is of relatively poor signal-to-noise,

having been observed through thin clouds. All of the apparent features in this spectrum can be attributed to imperfectly subtracted night-sky emission lines, leaving no definite intrinsic features in the 4600–9200 Å range.

5. A Transient X-ray Source in the Field of TeV J2032+4130

5.1. X-ray Properties

None of the X-ray sources in the immediate vicinity of TeV J2032+4130 are unusual in any way, except for *Chandra* source #2, which lies 7′ from the TeV centroid. Although this is the brightest of the *Chandra* sources, with 195 photons detected, it is noticeably absent from any of the *ROSAT* or *Einstein* images. Thus, it may be described as a transient source. A light curve constructed from the 5 ks *Chandra* observation shows that the source was highly variable even during this brief period (Figure 7). After remaining faint for the first 3.5 ks, its count rate rose by about a factor of 10 for the final 1.5 ks.

Spectral analysis of source #2, summarized in Table 4, is consistent with a power law of photon index $\Gamma \sim 2.0$, or with a hot plasma of $kT \sim 6$ keV. In addition to spectral fits for the summed observation, Table 4 presents fits for two intervals, corresponding to the first 3438 s (low state) and the final 1478 s (high state). Figure 8 shows the spectrum and best fitted power law for the summed observation. For either spectral model, a significant absorbing column of $N_{\rm H} \sim (1-2) \times 10^{22}$ cm^{-2} is required, which is comparable to the largest X-ray and optical extinction values measured for stars in the Cyg OB2 association (MT91; Waldron et al. 1998). Thus, source #2 is likely to be either embedded in the Cyg OB2 association at $d = 1740$ pc (MT91), or behind it. Its peak 1–10 keV flux of $\approx 2 \times 10^{-12}$ ergs cm^{-2} s^{-1} would correspond to a luminosity of 7×10^{32} ergs s^{-1} at $d = 1740$ pc. This value is somewhat larger than even the most luminous cataclysmic variables (Eracleous, Halpern, & Patterson 1991), and hints at a more compact source such as a neutron star or black hole in a quiescent low-mass X-ray binary (LMXB), or a very distant Be transient. If so, its location could be considerably beyond Cyg OB2.

The transition in the light curve of #2 may be an egress from an eclipse, or, more likely for an LMXB, a "dip". If so, the orbital period is probably longer than a few hours since the eclipse or dip is at least 1 hr long. A possible analog would be 4U 1624–49, the "big dipper," which has period of 21 hr (Watson et al. 1985; Smale, Church, & Balucińska-Church 2001). However, assuming a distance of 8 kpc, the X-ray luminosity of #2 would be only 1.5×10^{34} ergs s^{-1}, much less than the $\sim 10^{38}$ ergs s^{-1} luminosity of 4U 1624–49.

5.2. Optical and Infrared Properties

As mentioned previously, the signal-to-noise ratio of the *HET* optical spectrum of the counterpart to source #2 is too poor to classify it. However, it is likely to be the correct identification because the X-ray and optical positions differ by only $0\farcs37$. The absence of strong TiO absorption bands rules out a late K or M dwarf, which would otherwise be the expected spectral type for a star of its magnitude and color located between us and the Cyg OB2 association. Additional evidence that it is a more distant and luminous object comes from its detection in the 2MASS survey, with $J = 15.41 \pm 0.07$, $H = 14.17 \pm 0.06$, and $K = 13.45 \pm 0.06$. The absence of Hα emission argues against a cataclysmic variable, as does the high-state X-ray luminosity of $\approx 7 \times 10^{32}\,(d/1.7\,\mathrm{kpc})^2$ ergs s^{-1}, although it cannot be ruled out that the optical spectrum is highly reddened emission from an accretion disk in a quiescent LMXB.

If we hypothesize a very large visual extinction of $A_V = 10$, which is compatible with the value of N_H fitted to the X-ray spectrum, then the dereddened magnitudes become $R = 12.9$, $J = 12.6$, $H = 12.3$, and $K = 12.3$ using the extinction curve of Cardelli, Clayton, & Mathis (1989). Such a flat color distribution would be compatible with accretion disk emission in an LMXB. Assuming a distance of 8 kpc, the corresponding absolute magnitude $M_R = -1.6$ is also in the range of LMXBs (van Paradijs & McClintock 1994). However, even at that large distance, the X-ray luminosity would be only 1.5×10^{34} ergs s^{-1}, and then it is not clear that the accretion luminosity would dominate over the secondary star in the optical. Also, such a source would fall far from the relation between absolute magnitude, X-ray luminosity, and orbital period in LMXBs delineated by van Paradijs & McClintock (1994), having too small an X-ray luminosity.

Alternatively, if the distance and extinction are even larger, then it could be an early type star such as a B star in a transient high-mass X-ray binary system. However, the absence of Hα emission argues against a Be star. Thus, there are no entirely satisfactory explanations of source #2 in terms of any type of X-ray binary.

5.3. A Proton Blazar?

While an AGN classification for the optical spectrum of source #2 cannot be immediately dismissed, the absence of any emission lines would favor a BL Lac identification, for which the lack of radio emission is highly unusual. Also, the known TeV blazars are highly episodic emitters, which is contrary to the steady nature of TeV J2032+4130. Thus, it would not be a simplification to hypothesize that #2 is an AGN. Nevertheless, it has long been

hypothesized that a class of radio-quiet blazars could exist (Mannheim 1993; Schlickeiser 1984) that are dominated by accelerated hadrons. In this "proton blazar" model, γ-ray emission arises from proton-induced cascades, and radio emission can be reduced if the ratio of accelerated electrons to protons is small. Alternatively, an extreme blazar whose synchrotron emission peaks at MeV energies, and inverse Compton at TeV energies, could be relevant (Ghisellini 1999). Because HEGRA performed a sensitive survey of the Galactic plane (Aharonian et al. 2002b), it may not be so surprising if it turns out that the first TeV selected blazar is discovered there.

6. Discussion and Conclusions

Spectroscopic optical identifications of most of the brighter X-ray sources in γ-ray error boxes of TeV J2032+4130 and 3EG J2033+4118 are O stars in the Cyg OB2 association at $d = 1.7$ kpc, or foreground late-type stars. Those *Chandra* sources that are identified with faint optical counterparts in the range $R \approx 17 - 20$, are probably M dwarfs, while the optically undetected sources with $R > 23$ are the most X-ray absorbed, thus are likely background AGNs. The only unusual X-ray source in this field is a transient one that is the brightest source in the recent *Chandra* observation. It has a peak 1–10 keV luminosity of $\approx 7 \times 10^{32}\,(d/1.7\,\mathrm{kpc})^2$ ergs s^{-1}. An optical spectrum of its $R = 20.4$ possible counterpart has, albeit with modest signal-to-noise, no strong emission or absorption features. The hard X-ray spectrum, rapid variability, and red optical/IR colors of this object suggest that it is a distant, quiescent X-ray binary system. On the other hand, it may also be the prototype of a new kind of AGN previously hypothesized to exist, the "proton blazar." If so, its X-ray flaring behavior is a significant property, and related optical variability might be expected.

If we hypothesize that either TeV J2032+4130 or 3EG J2033+4118 is a point source, then we have a limited number of plausible point-source candidates at other wavelengths, perhaps only one. Without knowing the exact nature of *Chandra* source #2, it is not a compelling identification for either TeV J2032+4130 or 3EG J2033+4118, especially since it lies outside both of their 2σ localization regions. It is $7'$ from the centroid of the TeV source, while the 2σ position uncertainty of TeV J2032+4130 is given as $\approx 4\farcm8$. However, since we are faced with the first unidentified TeV source, it is worthwhile to pursue whatever additional observations are needed to determine the nature of this variable X-ray candidate and to assess the possibility of its connection with TeV J2032+4130, no matter how remote.

If TeV J2032+4130 is truly an extended source, then it need not be centered on a point source counterpart at other wavelengths. Benaglia et al. (2001) suggested that colliding winds from the Cyg OB2 #5 system and from other O stars in this association could be

responsible for the EGRET source 3EG J2033+4118. Aharonian et al. (2002a) summarized those arguments, and hypothesized two possible origins for extended TeV emission that may be displaced from its originating source of energy. One is that TeV emission could arise from π^0 decay resulting from hadrons accelerated in shocked OB star winds and interacting with a local, dense gas cloud. The other is inverse Compton TeV emission in a jet-driven termination shock, either from an as-yet undetected microquasar, or from Cyg X-3. Another reason to investigate the nature of *Chandra* #2 would be to find out if it could be such a jet source. We plan to pursue more detailed X-ray and optical studies of this source.

This publication makes use of data obtained from HEASARC at Goddard Space Flight Center and the SIMBAD astronomical database. It also makes use of data products from the Two Micron All Sky Survey, which is a joint project of the University of Massachusetts and the Infrared Processing and Analysis Center/California Institute of Technology, funded by the National Aeronautics and Space Administration and the National Science Foundation. This work was based in part on observations obtained with the Hobby-Eberly Telescope, which is a joint project of the University of Texas at Austin, Pennsylvania State University, Stanford University, Ludwig-Maximillians-Universität München, and Georg-August-Universität Göttingen. The Marcario Low-Resolution Spectrograph is a joint project of the Hobby-Eberly Telescope Partnership and the Instituto de Astronomia de la Universidad Nacional Autónoma de Mexico. R. M. acknowledges support from NSF grant PHY-9983836. E.V.G. is supported by NASA LTSA grant NAG 5-7935. *Chandra* studies of unidentified γ-ray sources is supported by SAO grants GO2-3071X and GO2-3082X to J.P.H.

REFERENCES

Aharonian, F., et al. 2002a, A&A, 393, L37

Aharonian, F., et al. 2002b, A&A, 395, 803

Benaglia, P., Romero, G. E., Stevens, I. R., & Torres, D. F. 2001, A&A, 366, 605

Butt, Y., et al. 2003, BAAS, 34, 1222

Caraveo, P. A. 2002, in High-Energy Gamma-ray Sources and the Quest for their Identification, Proc. XXII Moriond Astrophysics Meeting "The Gamma-Ray Universe" (Les Arcs, March 9–16, 2002), eds. A. Goldwurm, D. Neumann, and J. Tran Thanh Van, The Gioi Publishers (astro-ph/0206236)

Cardelli, J. A., Clayton, G. C., & Mathis, J. S. 1989, ApJ, 345, 245

Condon, J. J., Cotton, W. D., Greisen, E. W., Yin, Q. F., Perley, R. A., Taylor, G. B., & Broderick, J. J. 1998, AJ, 115, 1693

Daum, A., et al. 1997, APh, 8, 1

Eracleous, M., Halpern, J., & Patterson, J. 1991, ApJ, 382, 290

Ghisellini, G. 1999, APh, 11, 11

Halpern, J. P., Camilo, F., Gotthelf, E. V., Helfand, D. J., Kramer, M., Lyne, A. G., Leighly, K. M., & Eracleous, M. 2001a, ApJ, 552, L125

Halpern, J. P., Eracleous, M., Mukherjee, R., & Gotthelf, E. V. 2001b, ApJ, 551, 1016.

Halpern, J. P., Gotthelf, E. V., Mirabal, N., & Camilo, F. 2002, ApJ, 573, L41

Hartman, R. C., Bertsch, D. L., Bloom, S. D., Chen, A. W., Deines-Jones, P., Esposito, J. A., Fichtel, C. E., & Friedlander, D. P., et al. 1999, ApJS, 123, 79

Kaaret, P., Santina, P., Halpern, J. P., & Eracleous, M. 1999, ApJ, 523, 197

Lamb, R. C., & Macomb, D. J. 1997, ApJ, 488, L872

Mannheim, K. 1993, A&A, 269, 67

Massey, P., & Thompson, A. B. 1991, AJ, 101, 1408 (MT91)

Mattox, J. R., Hartman, R. C., & Reimer, O. 2001, ApJS, 135, 155

McLaughlin, M. A., Mattox, J. R., Cordes, J. M., & Thompson, D. J. 1996, ApJ, 473, 763

Mirabal, N., & Halpern, J. P. 2001, ApJ, 547, L137

Mirabal, N., Halpern, J. P., Eracleous, M., & Becker, R. H. 2000, ApJ, 541, 180

Monet, D., et al. 1996, USNO–SA2.0, (Washington DC: US Naval Observatory)

Mukherjee, R., Gotthelf, E. V., Halpern, J., & Tavani, M. 2000, ApJ, 542, 740

Mukherjee, R., Halpern, J., Mirabal, N., & Gotthelf, E. V. 2002, ApJ, 574, 693

Roberts, M. S. E., Hessels, J. W. T., Ransom, S. M., Kaspi, V. M., Freire, P. C. C., Crawford, F., & Lorimer, D. R. 2002, ApJ, 577, L19

Schlickeiser, R. 1984, ApJ, 277, 277, 485

Smale, A. P., Church, M. J., & Balucińska-Church, M. 2001, ApJ, 550, 962

van Paradijs, J., & McClintock, J. E. 1994, A&A, 290, 133

Waldron, W. L., Corcoran, M. F., Drake, S. A., & Smale, A. P. 1998, ApJS, 118, 217

Wallace, P. M., Halpern, J. P., Magalhães, A. M., & Thompson, D. J. 2002, ApJ, 569, 36

Watson, M. G., Willingale, R., King, A. R., Grindlay, J. E., & Halpern, J. 1985, Space Sci. Rev., 40, 195

Table 1. *ROSAT* Sources in the Field of 3EG J2033+4118 and TeV J2032+4130

ROSAT Ident.	*Chandra* cross ref.	X-ray Position R.A.[a]	Decl.[b]	Optical Position R.A.[a]	Decl.[b]	Name	Spectral Type	B (mag)	V (mag)	R (mag)
a	. . .	20 32 18.1	+41 28 07	20 32 19.244	+41 27 57.37	. . .	G8V	15.4	. . .	15.0
b	. . .	20 32 41.5	+41 27 44	20 32 41.454	+41 27 43.51	. . .	M5Ve	16.8	. . .	15.8
c	18	20 32 16.1	+41 27 08	20 32 13.836	+41 27 12.33	Cyg OB2 #4	O7III((f))	11.42	10.23	10.2
d	. . .	20 33 03.9	+41 24 14	20 33 03.902	+41 24 08.48	. . .	. . .	16.4	. . .	16.9
e	25	20 31 36.5	+41 23 38	20 31 37.267	+41 23 36.01	MT91 #115	G6V	13.90	13.10	13.1
f	26	20 31 51.5	+41 23 21	20 31 51.319	+41 23 23.79	MT91 #152	G3V	13.40	12.74	13.1
g	. . .	20 33 14.0	+41 20 14	20 33 14.144	+41 20 22.00	Cyg OB2 #7	O3If	11.94	10.50	. . .
h	. . .	20 33 15.3	+41 18 47	20 33 15.077	+41 18 50.50	Cyg OB2 #8A	O5.5I(f)	10.08	8.99	9.1
i	. . .	20 32 22.7	+41 18 17	20 32 22.432	+41 18 18.85	Cyg OB2 #5	O7e	10.64	9.21	8.1
j	. . .	20 33 11.0	+41 15 07	20 33 10.733	+41 15 08.22	Cyg OB2 #9	O5Iab:e	12.61	10.78	. . .
k	. . .	20 32 41.4	+41 14 28	20 32 40.957	+41 14 29.30	Cyg OB2 #12	B5Iab:	14.41	11.40	. . .
l	. . .	20 32 32.1	+41 14 11	20 32 31.556	+41 14 08.48	MT91 #267	. . .	15.06	12.87	11.8
m	27	20 31 38.0	+41 13 21	20 31 37.504	+41 13 21.05	Cyg OB2 #3	O9:	11.50	10.35	9.3
n	. . .	20 33 09.4	+41 13 21	20 33 08.820	+41 13 18.00	MT91 #417	O4III(f)	13.59	11.5	9.3
o	. . .	20 33 02.3	+41 11 19	20 33 01.793	+41 11 11.41	MT91 #384	. . .	17.28	16.73	16.1
p	. . .	20 33 23.3	+41 09 07	20 33 23.477	+41 09 13.38	MT91 #516	O5.5V((f))	14.04	11.84	11.0
q	. . .	20 32 07.9	+41 08 37	20 32 07.330	+41 08 50.56	. . .	. . .	14.7	14.2	13.6
r	. . .	20 33 41.6	+41 08 01	20 33 42.036	+41 07 53.70	MT91 #615	. . .	12.2	11.51	11.2

[a]Units of right ascension are hours, minutes, and seconds.

[b]Units of declination are degrees, arcminutes, and arcseconds.

Table 2. *Chandra* Sources in the Field of TeV J2032+4130

Chandra Ident.	*ROSAT* cross ref.	X-ray Position[a] R.A.	Decl.	Counts[b] (< 2 keV)	Counts[b] (> 2 keV)	Optical Position[a] R.A.	Decl.	Name	*R* (mag)
1	. . .	20 31 56.426	+41 37 23.35	7	35	. . .		. . .	> 23.2
2	. . .	20 31 43.755	+41 35 55.17	77	118	20 31 43.739	+41 35 55.49	. . .	20.4
3	. . .	20 32 10.248	+41 35 10.21	4	10	20 32 10.219	+41 35 11.31	. . .	18.3
4	. . .	20 32 25.392	+41 34 01.92	16	4	20 32 25.346	+41 34 02.10	MT91 #249	12.2
5	. . .	20 32 05.328	+41 33 12.38	3	10	. . .		. . .	> 23.7
6	. . .	20 32 27.456	+41 32 50.78	3	10	. . .		. . .	> 23.7
7	. . .	20 31 51.855	+41 31 18.91	3	22	. . .		. . .	> 23.7
8	. . .	20 32 30.504	+41 31 01.74	6	5	20 32 30.412	+41 31 02.88	. . .	21.2
9	. . .	20 31 39.192	+41 30 18.00	9	2	20 31 39.104	+41 30 18.49	. . .	17.1
10	. . .	20 31 23.544	+41 29 48.77	13	9	20 31 23.573	+41 29 49.45	. . .	15.1
11	. . .	20 32 18.845	+41 29 32.42	20	15	20 32 18.812	+41 29 32.83	. . .	19.3
12	. . .	20 32 37.848	+41 28 52.39	10	9	20 32 37.831	+41 28 52.93	. . .	16.7:[c]
13	. . .	20 32 25.752	+41 28 42.53	8	7	20 32 25.731	+41 28 42.89	. . .	17.3
14	. . .	20 32 28.080	+41 28 28.52	3	19	20 32 28.027	+41 28 29.02	. . .	18.8
15	. . .	20 32 52.163	+41 28 15.92	10	14	20 32 52.206	+41 28 17.17	. . .	19.3:[c]
16	. . .	20 32 42.072	+41 27 48.13	17	1	20 32 42.014	+41 27 48.32	. . .	15.7
17	. . .	20 32 14.688	+41 27 39.67	7	8	20 32 14.693	+41 27 40.09	MT91 #221	12.0
18	*c*	20 32 13.843	+41 27 12.13	27	8	20 32 13.837	+41 27 12.34	Cyg OB2 #4	10.2
19	. . .	20 31 33.662	+41 26 51.46	15	22	20 31 33.650	+41 26 51.71	. . .	19.6
20	. . .	20 32 27.598	+41 26 21.62	20	3	20 32 27.663	+41 26 22.44	MT91 #258	10.4
21	. . .	20 32 45.432	+41 25 36.44	19	4	20 32 45.462	+41 25 37.51	Cyg OB2 #6	10.1
22	. . .	20 32 55.344	+41 25 17.00	15	8	20 32 54.773	+41 25 16.09	MT91 #360	16.2

Table 2—Continued

Chandra Ident.	*ROSAT* cross ref.	X-ray Position[a] R.A.	Decl.	Counts[b] (< 2 keV)	Counts[b] (> 2 keV)	Optical Position[a] R.A.	Decl.	Name	*R* (mag)
23	. . .	20 32 06.877	+41 25 10.61	23	26	20 32 06.826	+41 25 10.68	. . .	20.3
24	. . .	20 31 47.568	+41 24 48.02	12	15	20 31 47.535	+41 24 48.43	. . .	18.1
25	*e*	20 31 37.251	+41 23 35.44	29	3	20 31 37.267	+41 23 36.01	MT91 #115	13.1
26	*f*	20 31 51.321	+41 23 22.75	54	7	20 31 51.319	+41 23 23.79	MT91 #152	13.1
27	*m*	20 31 37.156	+41 13 17.42	169	59	20 31 37.504	+41 13 21.05	Cyg OB2 #3	9.3

[a]Units of right ascension are hours, minutes, and seconds. Units of declination are degrees, arcminutes, and arcseconds.

[b]Soft and hard counts in a 12″ radius aperture. The total included background is estimated as 1–3 counts.

[c]Crowded field.

Table 3. NVSS Sources in the Field of TeV J2032+4130

R.A.[a]	Decl.[b]	$F_{1.4\mathrm{GHz}}$ (mJy)
20 31 31.18	+41 25 12.6	2.1
20 31 45.08	+41 35 34.2	18.1
20 31 48.17	+41 33 58.3	6.1
20 31 56.81	+41 35 31.4	4.5
20 32 01.34	+41 37 22.7	14.0
20 32 08.33	+41 29 17.4	3.8
20 32 17.04	+41 26 21.4	2.3
20 32 52.27	+41 30 09.5	10.6

[a]Units of right ascension are hours, minutes, and seconds.

[b]Units of declination are degrees, arcminutes, and arcseconds.

Table 4. Spectral Fits to *Chandra* Source #2

Parameter	Total Interval	Faint Interval	Bright Interval
Counts (1–6 keV)	169	35	134
Exposure Time (s)	4916	3438	1478
Count Rate (s^{-1})	0.03	0.01	0.09
Power Law:			
$N_{\rm H}$ (10^{22} cm^{-2})	$1.5(0.6-2.3)^{a}$	1.3	1.7
Γ	$2.0(1.2-2.7)^{a}$	2.1	2.0
Flux (10^{-13} ergs cm^{-2} s^{-1})[b]	6.6	1.8	18.0
χ^2_ν(dof)	0.6(13)	1.0(2)	0.4(10)
Raymond-Smith:			
$N_{\rm H}$ (10^{22} cm^{-2})	$1.2(0.6-1.8)^{a}$	0.9	1.6
kT (keV)	$6.0(3.0-\infty)^{a}$	6.6	4.0
Flux (10^{-13} ergs cm^{-2} s^{-1})[b]	7.1	2.1	17.4
χ^2_ν(dof)	0.6(13)	1.1(2)	0.3(10)

[a] 1σ uncertainty range for two interesting parameters.

[b] Absorbed flux in the 1–10 keV energy band.

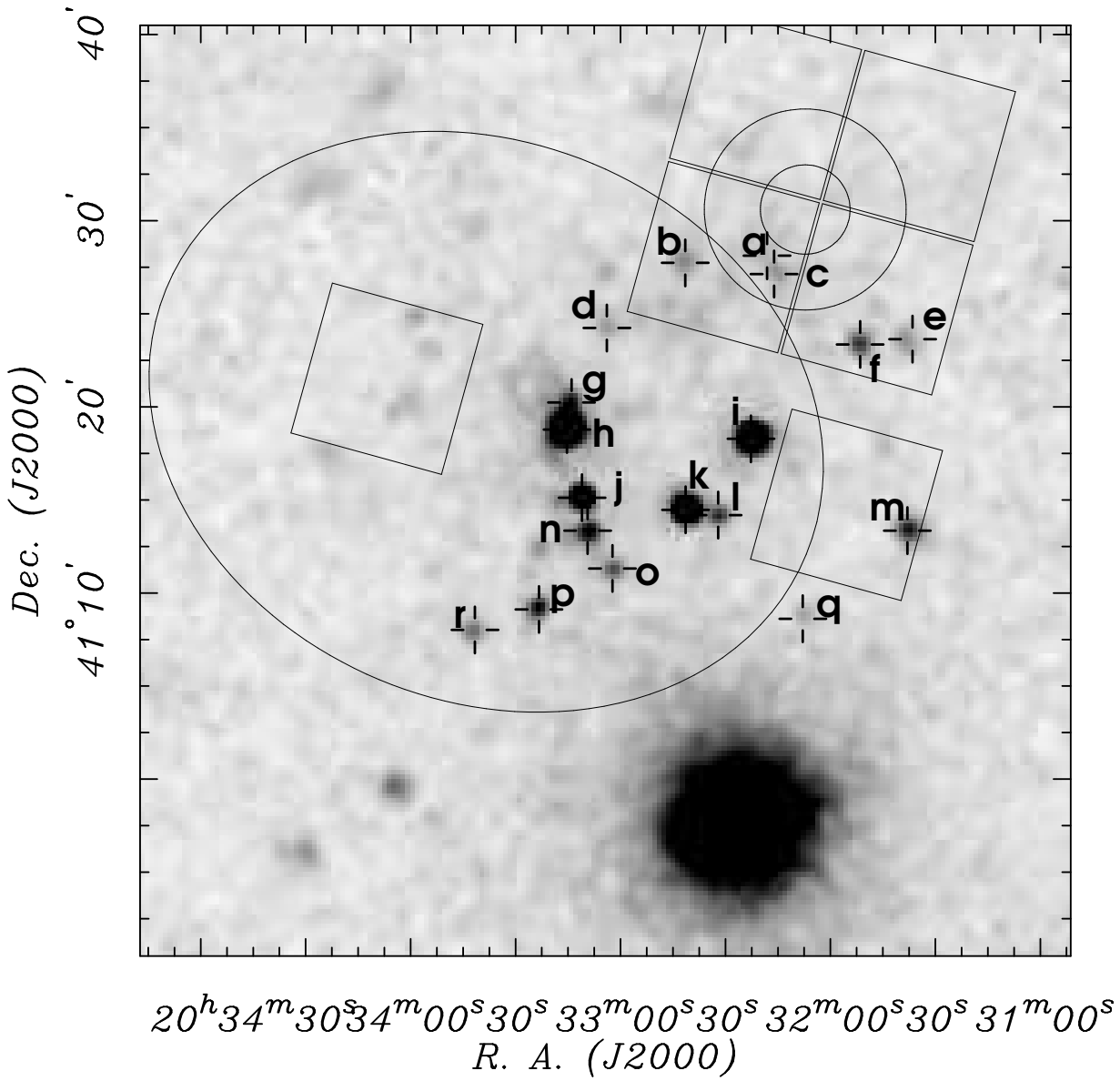

Fig. 1.— *ROSAT* PSPC X-ray image. The bright source is Cyg X-3. The properties of the numbered sources are given in Table 1. The ellipse is the 95% uncertainty location of 3EG J2033+4118 from Mattox et al. (2001). The small circle is the 1σ uncertainty of the centroid of TeV J2032+4130, and the large circle is the estimated Gaussian 1σ extent of the TeV emission (Aharonian et al. 2002a). The squares are the fields of view of the CCDs in the subsequent *Chandra* observation (see Figure 4).

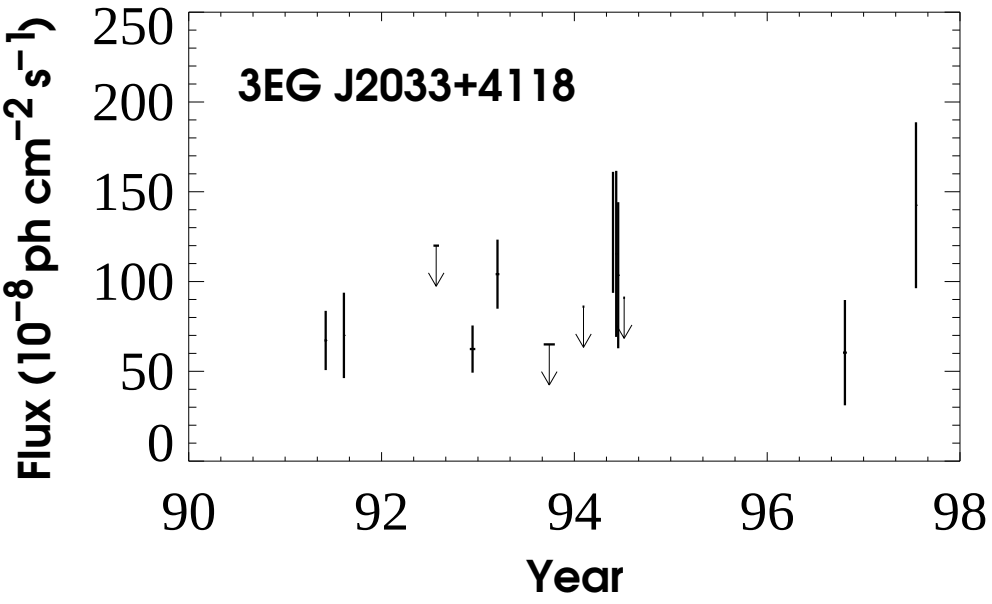

Fig. 2.— EGRET γ-ray light curve for 3EG J2033+4118, 1991–1995 from Hartman et al. (1999), and 1996–1997 from this paper. Arrows are 2σ upper limits. The horizontal error bars correspond to the extent of an individual observation.

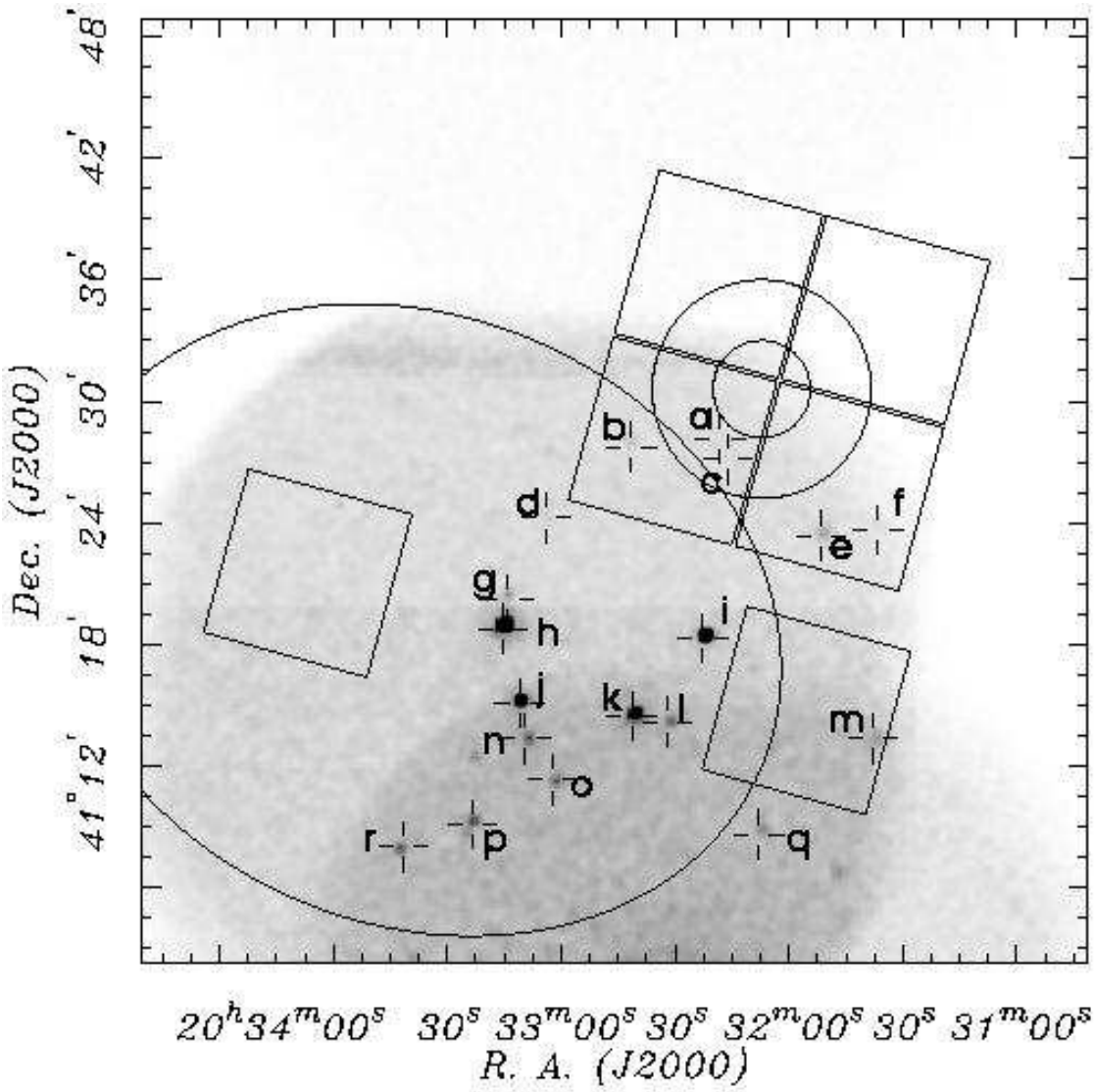

Fig. 3.— Same as Figure 1, but for the *ROSAT* HRI X-ray images in the field of 3EG J2033+4118 and TeV J2032+4130.

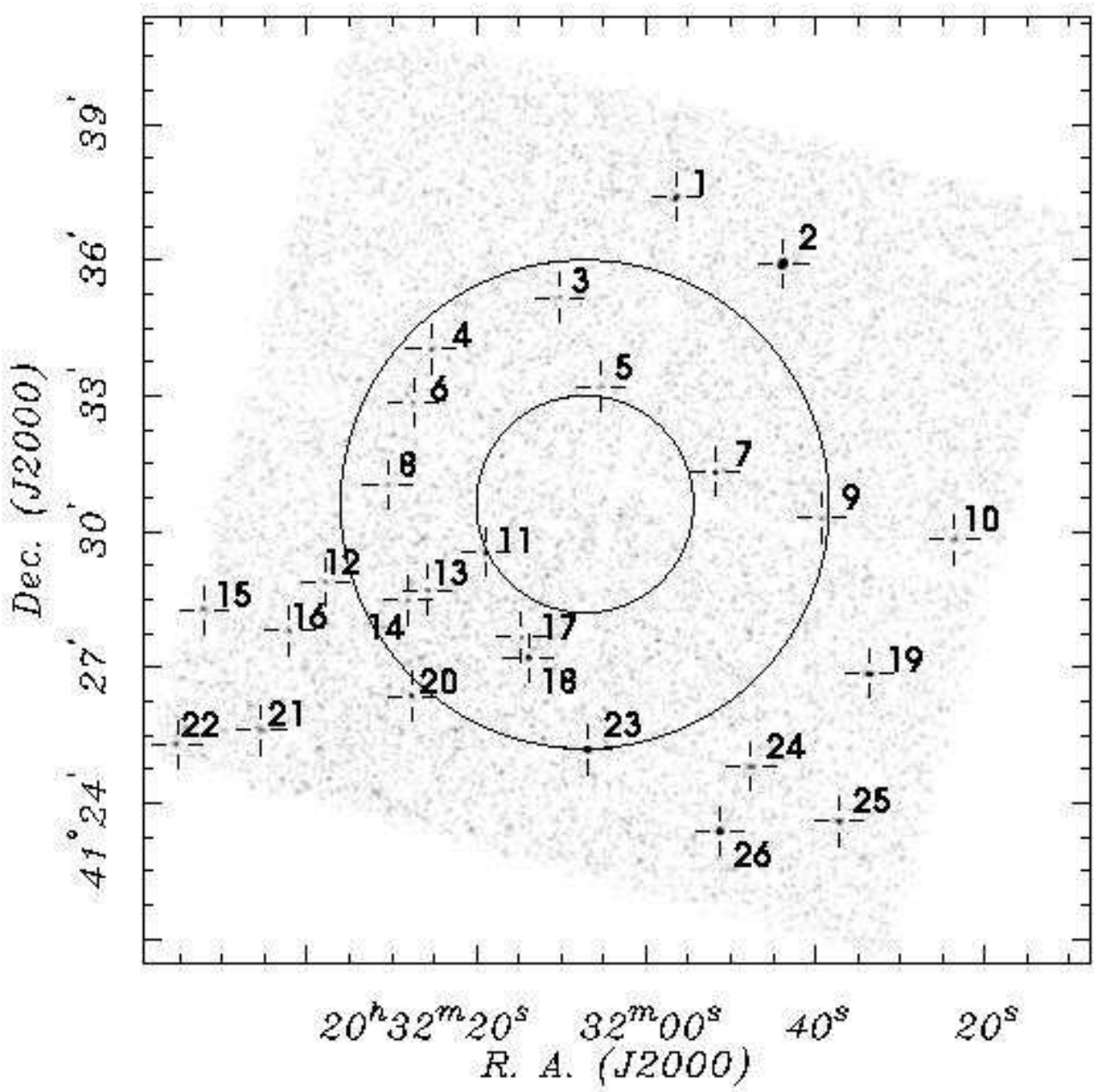

Fig. 4.— *Chandra* ACIS-I image of the field of TeV J2032+4130. The properties of the identified sources are given in in Table 2. The small circle is the 1σ uncertainty of the centroid of TeV J2032+4130, and the large circle is the estimated Gaussian 1σ extent of the TeV emission (Aharonian et al. 2002a). The brightest *Chandra* source #2 was not detected in *ROSAT* images.

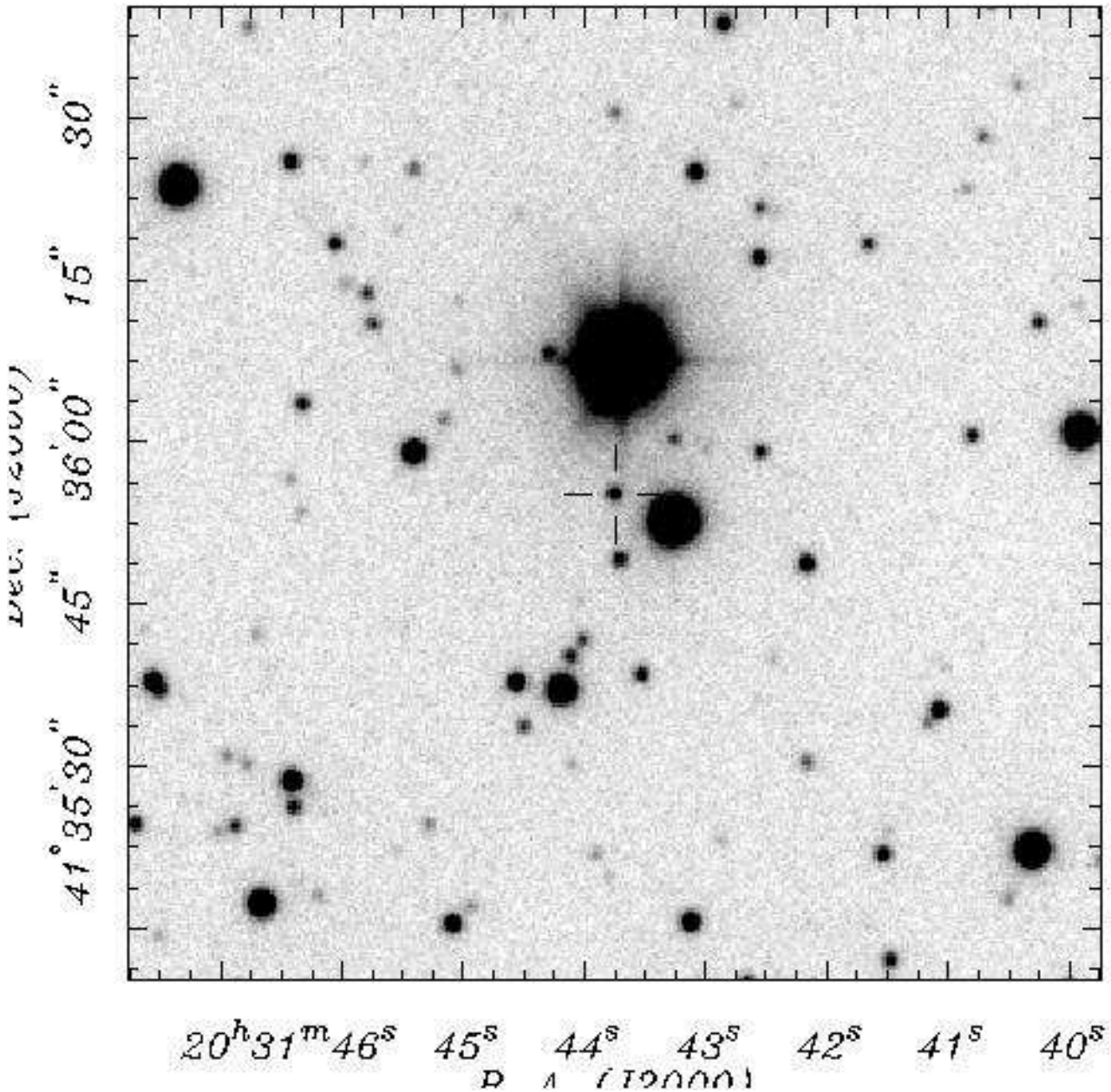

Fig. 5.— R-band finding chart for *Chandra* source #2 taken with MDM 2.4m telescope on 2002 November 24. Seeing is 1.″0. The *cross* marks the X-ray position, which is coincident with a star of magnitude $R = 20.4$.

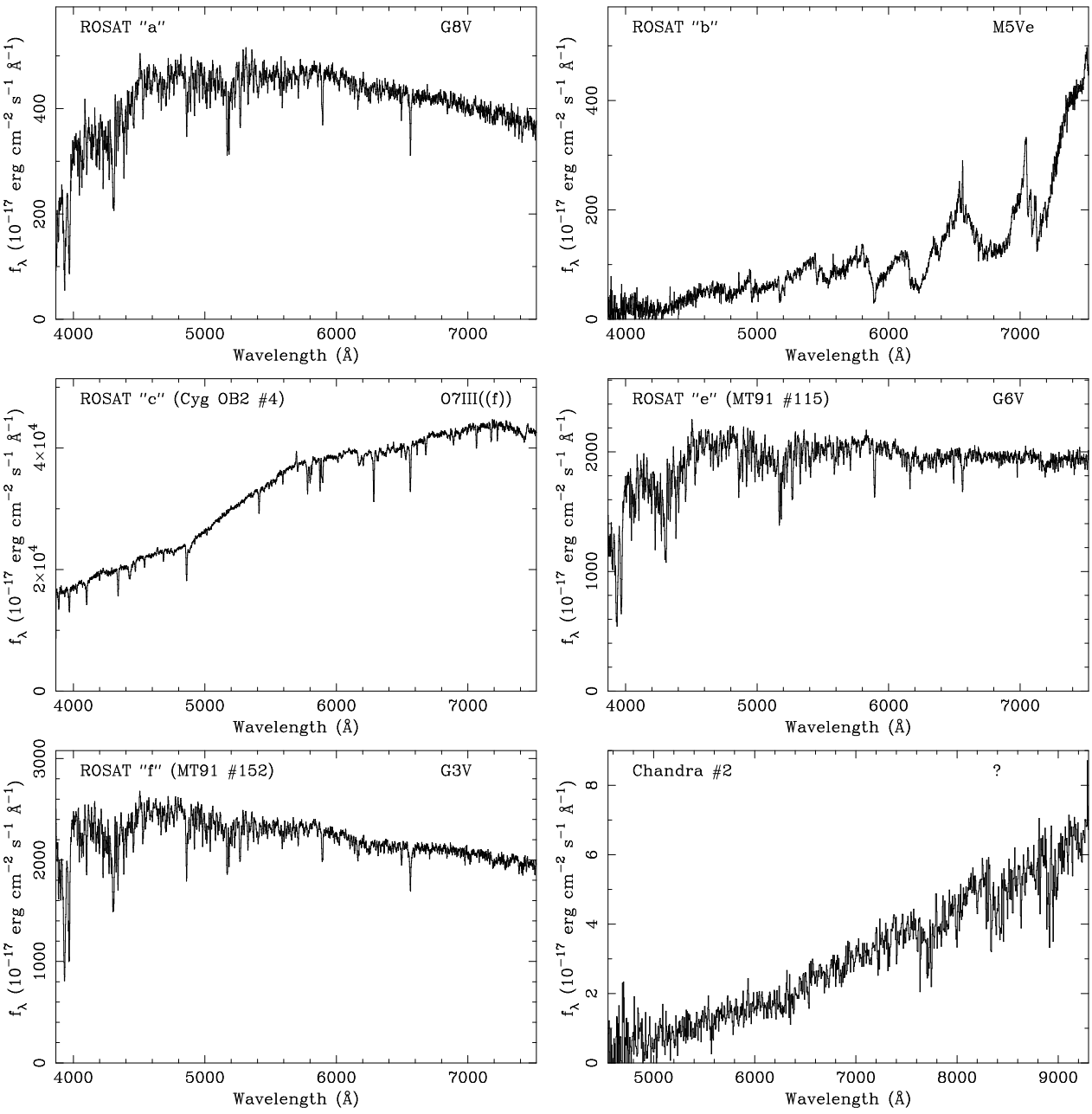

Fig. 6.— Optical spectra of five *ROSAT* sources in the field of TeV J2032+4130 taken with the KPNO 2.1m telescope, and one *Chandra* source with the *HET*.

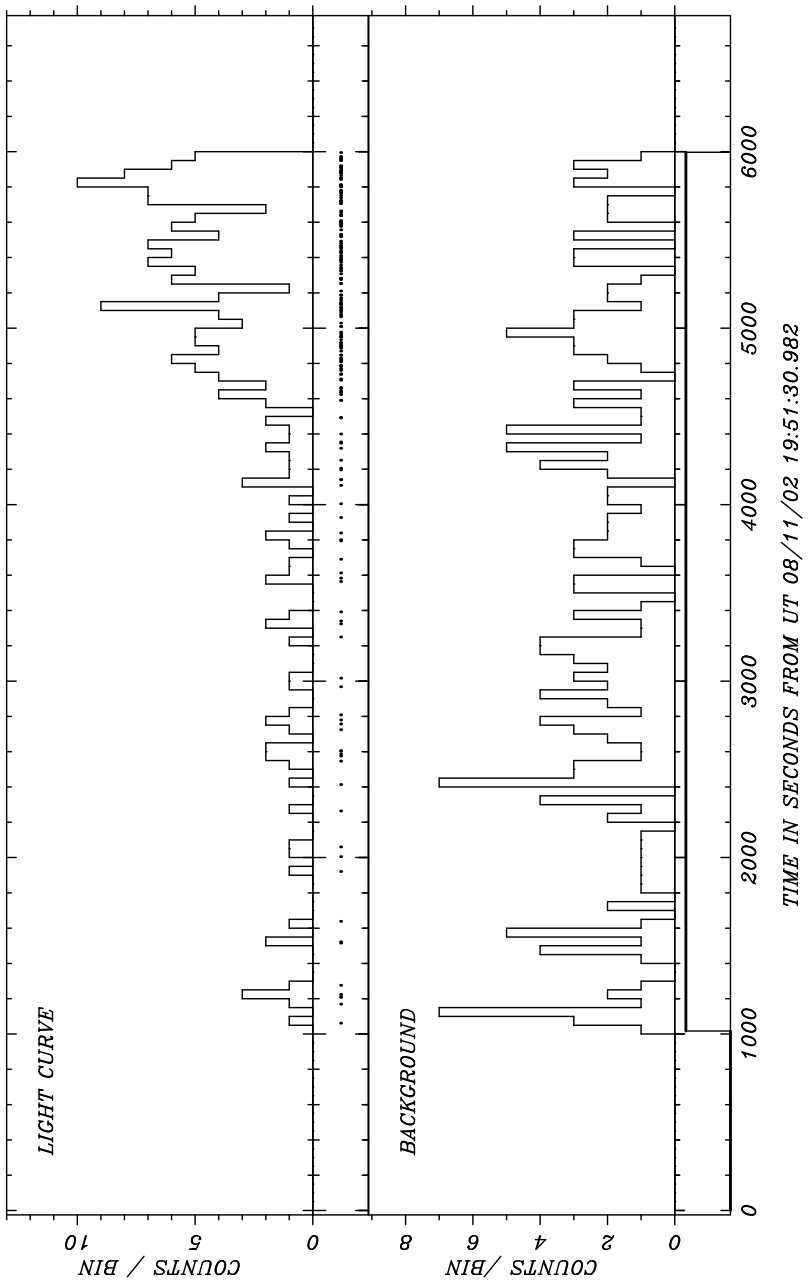

Fig. 7.— *Upper panel*: Light curve of *Chandra* source #2 extracted from an aperture of radius 12″, in 50 s time bins. The *dots* below the light curve are the arrival times of the individual photons. *Lower panel*: Local background extracted from an area 33 times larger than the source extraction region. Thus, background is demonstrated to be stable, and a negligible contaminant of the source light curve.

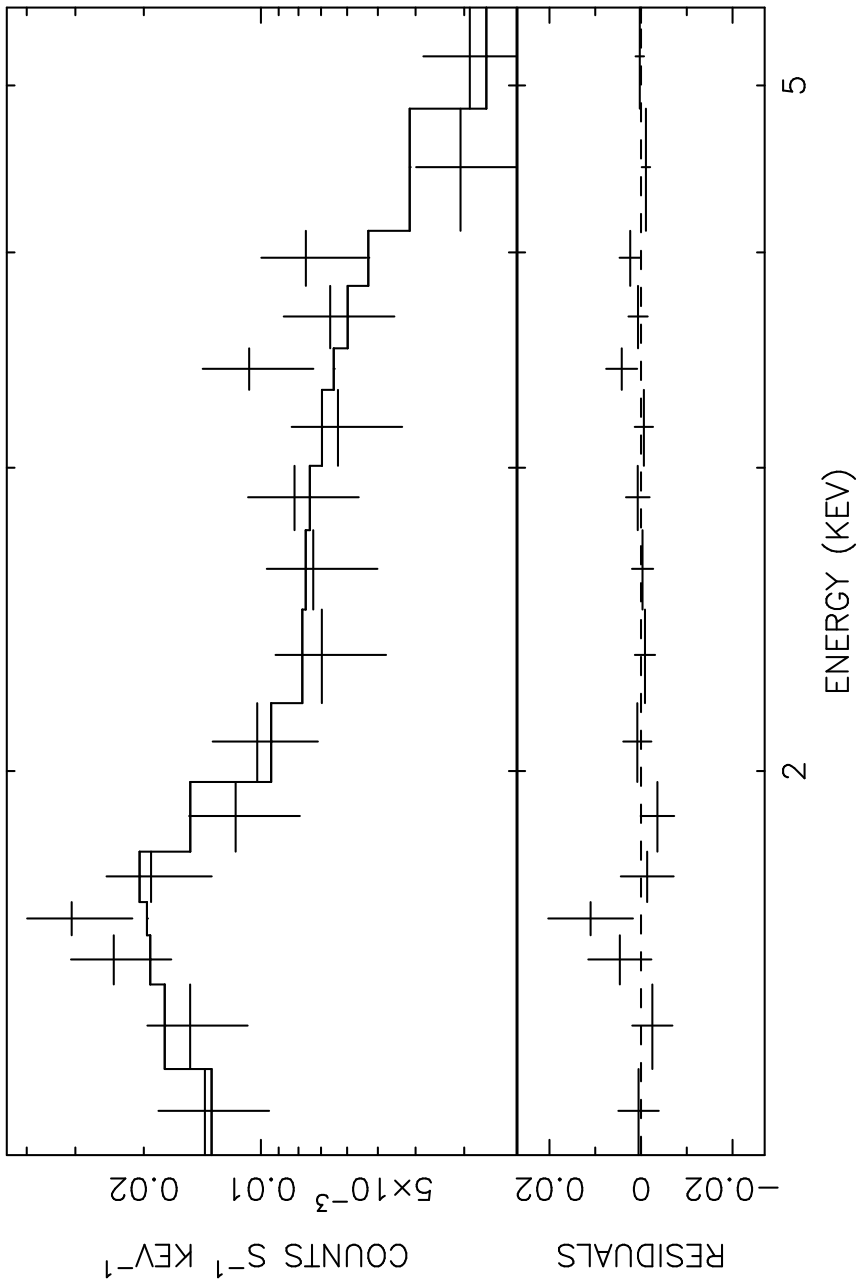

Fig. 8.— Spectrum of *Chandra* source #2 (*crosses*) and best fitted power-law model (*solid line*). This spectrum is for the entire time interval extracted from a 12″ radius aperture. The background is treated as negligible, as demonstrated in Figure 7.